Quasi-clamped Inductive Switching Behaviour of Power Mosfets

Sanjay Havanur, Principal Applications Engineer, Alpha & Omega Semiconductor, Inc.

Abstract - **Turn off behaviour of power Mosfets with Quasi-clamped Inductive Switching (QIS) loads is analysed. In most real applications the main inductive load is clamped during turn off but there is enough unclamped inductance in the circuit to cause voltage spikes and avalanche breakdown. This is the QIS situation and occurs in almost all practical circuits from motor drives to inverters to VRMs. Analytical expressions are derived for turn off losses under QIS which take into account the unclamped inductance in the circuit, gate drive parameters and more importantly, the source inductance of the package. The equations also predict the peak voltage during turn off and the conditions that would drive the device into avalanche.**

A common solution for avalanche prevention during inductive turn off is the protected Mosfet with an integrated drain to gate zener diode. The zener diode forces the Mosfet to turn on, thereby clamping the drain voltage. The trade offs in the design of such protected Mosfets are analysed. The findings are verified in the practical case of a power tool where the motor speed is controlled by PWM operation of a single switch. The circuit has large unclamped inductances arising from wiring and very high peak currents under locked rotor conditions. It is shown that a well designed Mosfet with avalanche protection can survive the locked rotor condition for longer durations, thereby increasing the overall product reliability.

INTRODUCTION

The inductive turn off of power devices has been analysed in detail, [1] – [6]. However the literature has concentrated on two extremes; one is the totally unclamped inductive switching, as in automotive applications where the device is allowed to go into avalanche with the specified load current by default, and survive. The other case, known simply as "inductive turn off" refers to the situation where the peak switch voltage is predictably clamped, either by topology as in a synchronous buck or an inverter, or by a snubber as in a flyback converter. By default there is no other unclamped inductance in the circuit. Fig 1) shows the conventional turn off waveforms.

The corresponding time intervals are

T_0 – Gate voltage fall time from V_{gs} to V_{gp}. No change occurs in V_{ds} or I_{ds}

T_{v_rise} – Plateau time at V_{gp}. Vds rises from a low saturated level to V_{in}. I_{ds} does not change

T_{i_fall} – Current falls from peak I_{ds} to 0A as V_{gs} falls from plateau voltage V_{gp} to gate threshold V_{th}

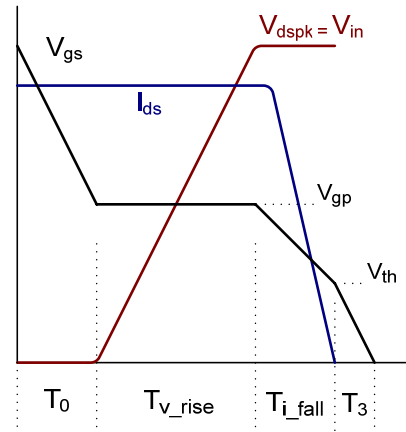T_3 – V_{gs} falls from V_{th} to zero. Turn off is complete.

Fig 1) Inductive turn off waveforms.

The reality is quite at variance with the simple model above. Practical measurements show that the current fall times are much longer than what the gate drive conditions predict. Given that there will always be some parasitic inductance in the circuit that lies outside the clamp, the peak voltage seen by the switch will be higher than V_{in} and complicated further by the resonant ringing of the circuit inductance with the output capacitance of the switch. A more practical analysis is needed taking into account parasitic inductances both in the circuit and the package to predict the turn off behaviour. The source inductance, in combination with total circuit inductance, influences not only the switching behaviour and the losses, but also the peak turn off voltage and avalanche breakdown. Fig 2) shows the Quasi-clamped Inductive Switching (QIS) circuit used in this analysis. L_{ckt} represents the parasitic circuit inductance that lies outside the freewheeling diode. Fig 3) shows the turn off waveforms with corresponding time intervals.
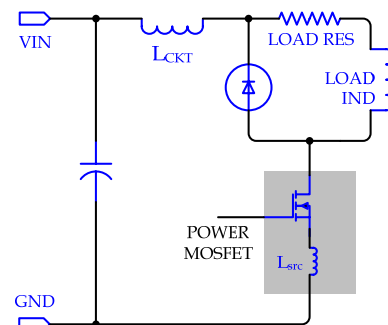

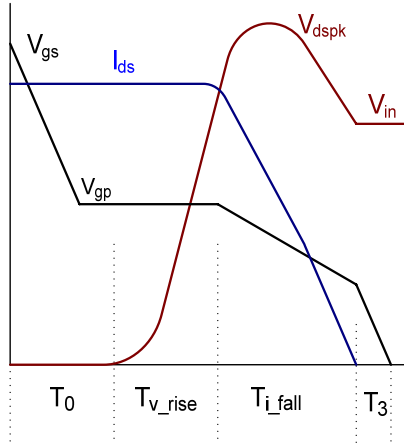Fig 2) Quasi-clamped Inductive Circuit

Fig 3) Switching waveforms for QIS

SWITCHING TIME CALCULATIONS DURING TURN OFF

Usually the voltage rise time is written in terms of the gate to drain Miller charge Q_{gd}. However it is found that Q_{gd} is not a reliable parameter to predict the voltage rise time. Fig 4) shows the simulation of a Mosfet turn off under normal gate drive conditions. During inductive turn off with large gate currents, bulk of the drain to source voltage V_{ds} transition is completed while the gate voltage is still at the Miller plateau. The standard test circuit for measuring Q_{gd} uses a much smaller gate current and does not provide a practically usable parameter. The alternative is to use reverse capacitance C_{rss}, which unfortunately varies considerably with V_{ds}. Empirical measurements have shown that a value of 2 x C_{rss} gives a better approximation of the rise time.

$$T_{v\_rise} = 2 \times C_{rss} \times V_{dspk} \times [(R_g + R_{snk})/ (V_{gs} - V_{gp}]$$

R_{snk} is the equivalent series resistance of the gate drive circuit and R_g is the internal gate resistance. V_{dspk} is the peak drain to source voltage reached during the inductive turn off conditions and is an unknown at this stage. The term in square brackets is the inverse of gate turn off current and may be considered to be constant during the interval.
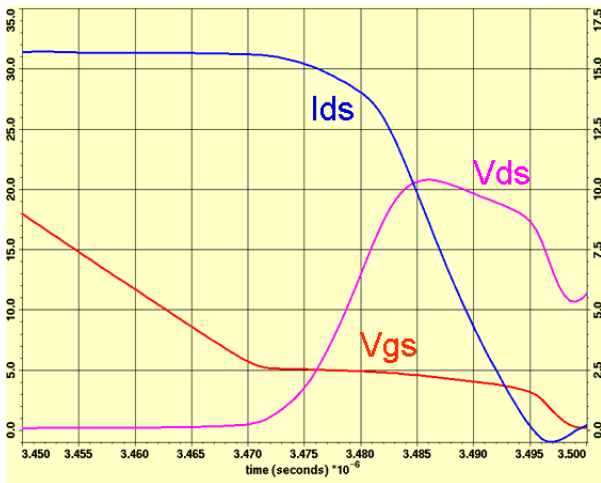

Fig 4) Turn off waveform simulations

Conventionally the current fall time is estimated as the time required by the gate to discharge from V_{gp} to V_{th}, [3] and written as

$$T_{i\_fall} = C_{iss} \times (R_g + R_{snk}) \times \ln (V_{gp} / V_{th})$$

In reality the measured current fall times are much longer. The anomaly is readily explained if it is realised that there are three possible expressions for calculating the current fall time.

- Gate turn off time expressed by

$$C_{iss} \times (R_g + R_{snk}) \times \ln (V_{gp} / V_{th})$$

- di/dt of the circuit inductance, expressed by

$$(V_{dspk} - V_{in}) / L_{ckt}$$

L_{ckt} is the total parasitic inductance in the circuit and can be estimated using the method in [7].

- Modified gate turn off time with package source inductance L_{src} taken into account

The idealised "inductive switching" analysis assumes no parasitic inductances and clamps V_{dspk} to V_{in}. This is of little practical value. Without this assumption we can write a generic expression for V_{dspk} as

$$V_{dspk} = V_{in} + L_{ckt} \times di/dt \qquad (1)$$

A simplifying assumption made in this analysis is that the current falls linearly from I_{ds} to zero i.e. V_{dspk} is constant during the current fall. If the fall time is dominated entirely by parasitic inductances,

$$di_{ds} / dt = I_{ds} / T_{i\_fall}$$
$$= (V_{dspk} - V_{in}) / L_{ckt} = V_{src} / L_{src}. \qquad (2)$$

The critical parameter now is V_{src}, the voltage across source inductance within the package, and given by $L_{src} \times di_{ds} / dt$. Realising that di/dt is same for source as well as circuit inductances is the key to solving for V_{dspk}. The presence of source inductance and its voltage V_{src} extends the gate transition time from V_{gp} to V_{th}, which is also the current fall time. The modified expression for gate turn off and T_{i_fall} is,

$$T_{i\_fall} = C_{iss} \times (R_g + R_{snk})$$
$$\times \ln [(V_{gp} - V_{src}) / (V_{th} - V_{src})] \qquad (3)$$

Eliminating T_{i_fall} from (2) and (3) gives us two expressions for V_{dspk} and V_{src}

$$V_{dspk} = V_{in} + (L_{ckt} / L_{src}) * V_{src} \qquad (4)$$

This is the circuit inductance based solution. The next expression can be described as the gate drive based solution and written as

$$V_{dspk} = \qquad (5)$$
$$V_{in} + \frac{L_{ckt} \times I_{out}}{C_{iss} \times (R_g + R_{snk}) \times \ln [(V_{gp} - V_{src}) / (V_{th} - V_{src})]}$$

Despite the logarithmic term in the denominator, equations (4) and (5) can be solved for V_{src} and V_{dspk}, using simple numerical methods. Note that V_{dspk} has an upper limit at the avalanche breakdown voltage BV_{ds}, typically 1.3 times the V_{ds} rating of the device. The source voltage V_{src} also has an upper limit at the gate

threshold V_{th}. We can evaluate equations (4) and (5) for a range of assumed V_{src} values from 0 to V_{th}. The solution is that value of V_{src} where equation (4) and (5) yield the same result for V_{dspk}. In other words the *peak turn off voltage as well as current fall time should be same whether they are calculated using circuit inductances or by gate turn off expressions.* Once V_{dspk} is found, T_{i_fall} can be estimated from equation (3) and the turn off loss can be written as

$$P_{swoff} = \tfrac{1}{2}\, V_{dspk} \times I_{out} \times (T_{v\_rise} + T_{i\_fall}) \times F_{sw} \qquad (6)$$

The effect of source inductance has been covered in several application notes and papers, [8]–[11]. It is generally agreed that larger source inductance causes less V_{dspk}, reduced ringing and shoot through, but at the same time increases the turn off switching loss. Equations (3) to (6) above explain why it is so.

EXPERIMENTAL VERIFICATION

As an example the turn off behaviour of a power device AOT430 in TO-220 package was studied in a power tool application. This device has a $C_{iss} = 4.7$ nF, effective $V_{th} = 3.0$V and V_{ds} rating of 75V with an expected avalanche breakdown just below 100V. The typical drain to source R_{ds} value is 11 mΩ. During the tests input voltage, switching current and frequency and duty ratio were set to 24V, 10 kHz and 70% respectively. These were intended to duplicate the combination of worst case stresses such as the locked rotor condition, seen in the power tool. On the bench set up turn off waveforms were captured over a range of circuit inductances and peak currents and compared with predicted values.

A source inductance value of 12.5 nH was used in the calculations, of which 7.5 nH comes from within the TO-220 package and the rest from mounting with uncut leads. Gate turn off current was measured during T_{i_fall} and a gate series resistance of 10Ω was estimated. A spreadsheet was written to calculate the V_{dspk} during turn off as a function of drop across the source inductance using both gate drive conditions and di / dt in the circuit inductance. The operating point is where the two curves intersect, within the limits imposed by V_{th} and BV_{ds}. Depending on operating conditions two other solutions are possible. If the curves do not intersect even at $V_{src} = V_{th}$, the current fall is dominated by the parasitic inductance and gate drive has very little influence on it. At the other extreme, with large circuit inductances and/or fast gate drives the device will go into avalanche, indicated by a region where both curves will share a common value of BV_{ds}.

Figs 4a) and b) show calculated and measured results for a circuit inductance of 150 nH. The turn off is dominated by circuit inductance which clamps the V_{src} at its maximum of 3V. If the current is reduced to 50A, the two curves do intersect and the results are shown in Figs 5a) and 5b). Note that the V_{gs} waveform includes the source inductance voltage inside the package, which is almost equal to V_{th} because of the large parasitic inductances that were introduced in the circuit.
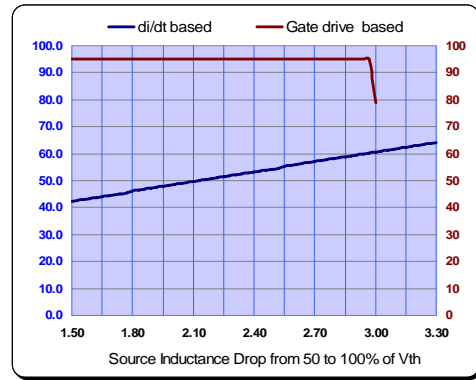

Fig 4a)   Calculation of V_{dspk} with $L_{ckt} = 150$ nH and $I_{ds} = 100$A
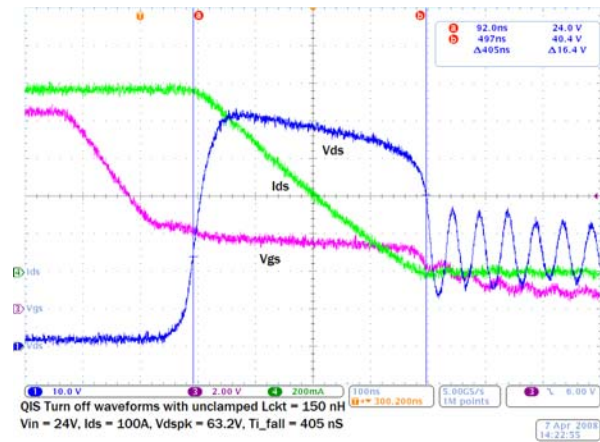

Fig 4b) QIS Turn off waveforms with $L_{ckt} = 150$ nH and Ids = 100A
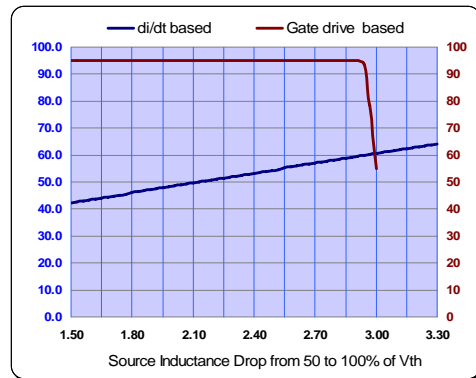

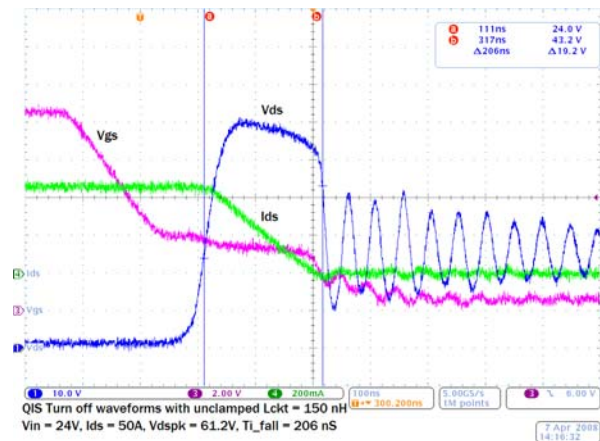Fig 5a)   Calculation of V_{dspk} with $L_{ckt} = 150$ nH and $I_{ds} = 50$A

Fig 5b) QIS Turn off waveforms with $L_{ckt} = 150$ nH and Ids = 50A
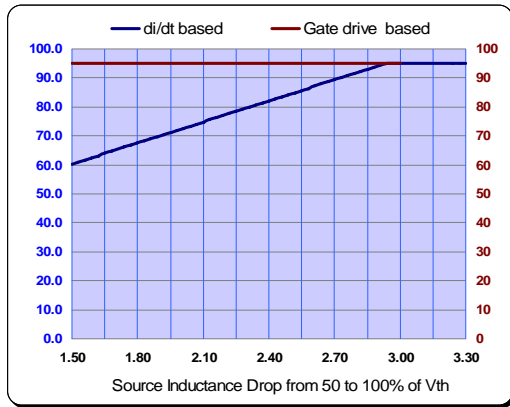
Fig 6a)   Calculation of V_{dspk} with L_{ckt} = 300 nH and I_{ds} = 100A

TABLE I: PEAK V_{ds} AND CURRENT FALL TIME CALCULATIONS

Vds Condition	Lckt	Iout	Vdspk		Tifall	
			Calc	Meas	Calc	Meas
	nH	Amp	Volts		nS	
Unclamped	70.0	100	41.2	**43.4**	348	**371**
		50	41.2	**42**	174	**185**
Unclamped	150.0	100	60.2	**63.2**	386.4	**405**
		50	60.2	**61.2**	193.2	**206**
Unclamped	250.0	100	84	**85.6**	400	**438**
		50	84	**82.4**	200	**232**
Avalanche	300.0	100	95.9	**96.8**	403.5	**464**
		50	95.9	**95.2**	201.7	**247**
Lsrc added to avoid avalanche	300.0	100	84.4	**85.2**	480	**514**
		50	84.4	**83.2**	240	**274**

Table I above lists the calculated and measured values over the full range of circuit inductances and peak currents. The correlation between calculation and measured data improves with higher values of L_{ckt} and V_{dspk}. The reason is that calculations assume a constant V_{dspk} and predict its average value. As V_{dspk} approaches BV_{ds} it gets flatter, justifying the assumption.

So long as V_{ds} is not clamped, the current fall time does not change much and di/dt rate remains within 10% of the calculated value of 260 A/uS. If T_{i_fall} were calculated using the standard gate drive based equations, without accounting for source inductance, the predicted fall time would be 5.1 nS.
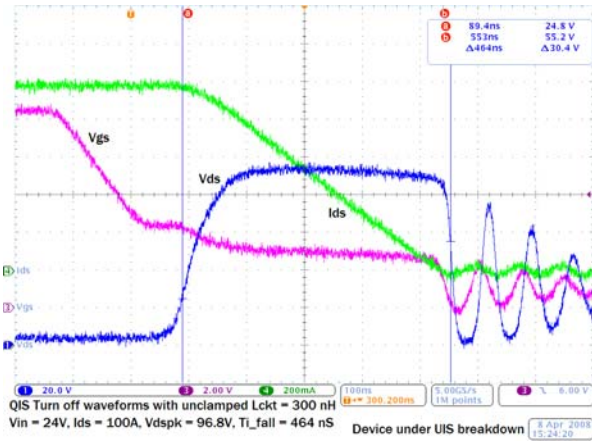

Fig 6b) QIS Turn off waveforms with L_{ckt} = 300 nH and I_{ds} = 100A.

Figs. 6a) and 6b) above show the results for circuit inductance of 300 nH. Avalanche breakdown is predicted, as seen by the upper BV_{ds} limit in Fig 6a), and observed in Fig. 6b). A simple variation can be tried to demonstrate the role source inductance plays in determining the peak V_{ds} and the avalanche condition. With 300 nH inductance still in place, a very short wire was added to source lead increasing L_{src} by no more than 2-3 nH. Calculations predict that the peak voltage should drop by about 10V, avoiding the avalanche breakdown but current fall time will increase as a result. Fig 7) shows the actual waveforms that confirm the analysis.
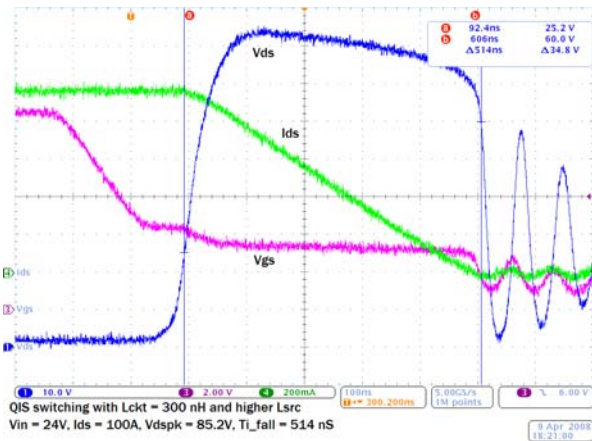
VOLTAGE CLAMPING

A common solution to the problem of excessive ringing and avalanche breakdown is to clamp the V_{ds}. If the clamp voltage is below the Mosfet breakdown limit, the device will not go into avalanche mode under any condition. However any attempt to clamp the peak voltage will invariably result in higher switching losses due to extended current fall times. Lower clamp voltages will result in successively longer turn off times and losses. Fig 8) shows an extreme case where the V_{dspk} is clamped close to the supply voltage
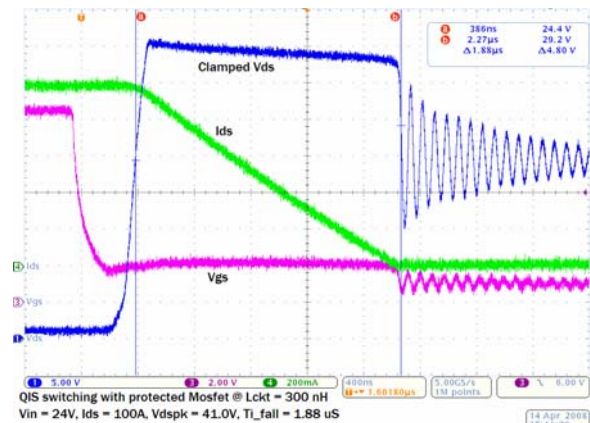

Fig 7) QIS Turn off waveforms with L_{ckt} = 300 nH and I_{ds} = 100A.
Avalanche avoided by increasing L_{src} to 15 nH.

Fig 8) QIS Turn off waveforms with L_{ckt} = 300 nH and V_{ds} clamping
close to supply voltage.

TABLE II: EFFECT OF V_{ds} CLAMPING ON CURRENT FALL TIME

Condition	Iout	Vdspk	Tifall
	Amp	Volts	nS
Vds under avalanche	100	96.8	464
	50	95.2	247
Vds clamped to 60V	100	59.6	895
	50	59.6	450
Vds clamped to 40V	100	41	1880
	50	40.6	924
Lckt = 300 nH, Ids = 100A peak			

Fig 10) Graphical representation of protected Mosfet.

Table II above shows the effects of clamp voltage vs. T_{i_fall}. The contribution to turn off losses from current fall time in equation (6) is $\frac{1}{2} V_{dspk} \times I_{out} \times T_{i\_fall} \times F_{sw}$.

This can be written as

$$P_{swi\_fall} = \frac{1}{2} L_{ckt} \times I_{out}^2 \times [\ 1 + V_{in} / (V_{dspk} - V_{in})\ ] \qquad (7)$$

The switching losses are at their lowest as long as the drain voltage is allowed to reach the natural peak demanded by the circuit, and increase inversely as the drain voltage is clamped closer to V_{in}. Notice that in Fig 7) with the device forced to operate below avalanche the current fall time has increased to over 500 nS. Clamping the peak voltage lower and closer to V_{in} will make the current fall time and losses much worse.

Despite the additional loss, there are applications where clamping the Mosfet may be the best option to avoid the avalanche breakdown and the associated latch up failures. One example is the PWM chopper for motor control used in a power tool. The basic block diagram is shown in Fig 9). The controller is a simple open loop circuit, implemented with logic gates or a timer like 555. The brake is a mechanical switch turned on to short the motor winding when the speed is set too low or turned off altogether. If the trigger speed is set >70%, the Mosfet is bypassed and battery is connected directly across the motor. Because of constructional constraints, the battery is located a few centimeters away from the Mosfet and the wiring can result in unclamped parasitic inductances as high as 500 nH. When the rotor is locked, large peak currents flow through the motor and the device, causing overshoots and/or avalanche breakdown.
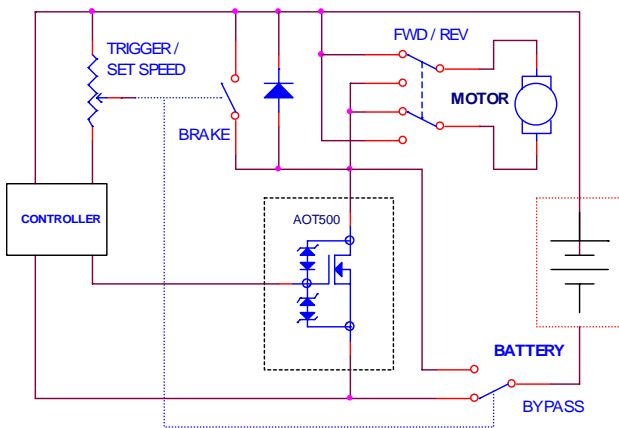

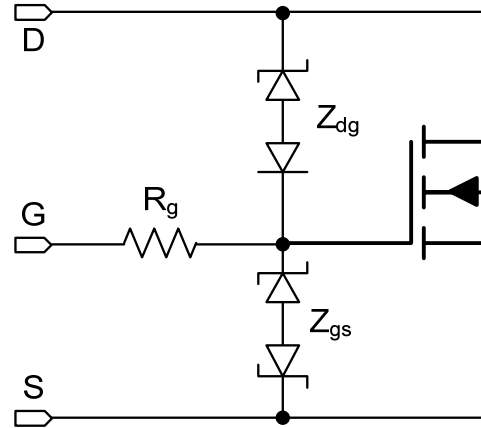Fig 9) Electrical block diagram of a power tool

PROTECTED MOSFETS

It is clear that the optimum design of Mosfet for such applications will require several trade offs, not the least of which is the overall cost. One such solution is a protected Mosfet. There are different levels of protections that can be bundled with a standard Mosfet package, such as overload, overtemperature and overvoltage. But for this application it was decided to put only a peak voltage clamp as shown in Fig 10). During turn off the V_{dspk} will now be clamped to the zener voltage $V_{zdg} + V_{th}$, which obviously will be lower than BV_{ds}. The gate resistance is chosen to ensure that turn on threshold is reached even with gate pin grounded. The aim is to activate the device and allow it to absorb the parasitic energy through the channel. Power handling capability during inductive turn off will now come not from UIS rating but forward biased SOA which is much higher.

The next trade off is to determine the actual voltage ratings for the zeners as well the Mosfet. For a given die size and cost, reducing the voltage rating can exponentially cut down the R_{ds} and the reduction in conduction loss can make up for the increased switching losses. Another benefit is that the normal operating efficiency will also improve due to lower R_{ds}, extending the battery life. With these considerations, various design choices were evaluated and the clamp was chosen at 40V for the protected Mosfet AOT500. Compared to the 75V 11 mΩ device, the protected version with the same die size has only half the R_{ds} value. The turn off waveforms shown in Fig 8) came from this protected Mosfet.

Since the ability to survive the locked rotor condition for extended durations is the single most important benchmark of Mosfet performance in a power tool, the new protected device was compared with several others in that respect. Each Mosfet was attached to a small heatsink and allowed to switch high peak currents in the range of 60A to 80A continuously at 10 kHz with 18V and 24V input till they failed. The time to fail as well as the junction temperature were measured using a thermal camera. The results are shown in Table III. It is seen that the clamped Mosfet, despite the increased switching losses is more reliable, in that it lasts longer under extreme conditions.

TABLE III: PERFORMANCE OF THE PROTECTED MOSFET
UNDER HIGH CURRENT CONDITIONS

Ids	DUT	Vdspk	Duration	Tj	Result
60A	AOT430	92V	9 S	230 °C	Fail
60A	AOT500	40V	22 S	213 °C	Pass
75A	AOT500	40V	7 S	240 °C	Fail

In addition to bench testing, the protected Mosfet was installed in a commercial power tool with an 18V, 1.7 AH battery pack. Two Mosfets were operated in parallel, and the locked rotor condition was maintained till the battery was fully discharged and the motor was shut off. For safety reasons it is specified that the power tool remain operational for at least 20 seconds under locked rotor conditions. The results show the requirement being met with adequate margin.

TABLE IV: PERFORMANCE OF THE PROTECTED MOSFET
IN AN ACTUAL POWER TOOL

Vdspk	Ids	Freq	Duty	Time
Volts	Amps	kHz	%	Seconds
39.4	88	7.4	65.9	35.2
39.2	93	6	69.7	34.8
39.4	92	6.6	69.6	35.7
39.2	91	7.2	65.7	35.9
Note: Ids is the initial value of the peak current, which reduces over time as the battery discharges				

REFERENCES

[1] R. Erickson and D. Maksimovic, "Fundamentals of Power Electronics", Kluwer Academic Publishers, Second Edition, 2001, Chapter 4, pp 92-96.

[2] Peter Markowski, "Estimating MOSFET switching losses means higher performance buck converters", [Online] http://www.planetanalog.com/showArticle.jhtml?articleID=12802296

[3] J Brown, "Modeling the Switching Performance of a MOSFET in the High Side of a Non-Isolated Buck Converter", IEEE Trans on Power Electronics, Vol. 21, No. 1, January 2006, pp 3-10

[4] Yuancheng Ren, Ming Xu, Jinghai Zhou, and Fred Lee, "Analytical Loss Model of Power MOSFET" IEEE Transactions on Power Electronics, Vol. 21, No. 2, March 2006, pp 310 -319

[5] Shen Z.J., Yali Xiong, Xu Cheng, Yue Fu and Kumar P., "Power MOSFET Switching Loss Analysis: A New Insight", IEEE Industry Applications Conference 2006, Vol. 3, pp 1438-1442

[6] Toni Lopez and Reinhold Elferich "Quantification of Power MOSFET Losses in a Synchronous Buck Converter", IEEE Applied Power Electronics Conference, APEC 2007 Vol. 3, pp 1594-1600

[7] Sanjay Havanur, "Snubber Design for Noise Reduction in Switching Circuits" Alpha and Omega Semiconductor Application Note AN-100, May 2007, www.aosmd.com

[8] Qun Zhao, Goran Stojcic, "Characterization of Cdv/dt Induced Power Loss in Synchronous Buck DC-DC Converters", IEEE Applied Power Electronics Conference, APEC 2004, Vol. 1, pp 292 – 297.

[9] Bo Yang, Jason Zhang "Effect and Utilization of Common Source Inductance in Synchronous Rectification", IEEE Applied Power Electronics Conference, APEC 2005, Vol. 3, pp 1407 – 1411.

[10] F Merienne, J Roudet, J.L. Schanen, "Switching disturbance due to source inductance for a power MOSFET: analysis and solutions", IEEE Power Electronics Specialists Conference, PESC 1996 Record, Vol. 2, pp 1743 – 1747

[11] W Teulings, J.L. Schanen, J Roudet, "MOSFET Switching Behaviour Under Influence of PCB Stray Inductance", IEEE Industry Applications Conference, 1996. Vol. 3, pp 1449 – 1453.